Enhanced photoluminescence efficiency of mid-infrared InAsSb nanostructures using a carrier blocking layer

W. Lei,[a] H. H. Tan, and C. Jagadish
Department of Electronic Materials Engineering, Research School of Physics and Engineering, The Australian National University, Canberra ACT 0200, Australia

(Received 3 April 2010; accepted 4 May 2010; published online 24 May 2010)

This paper presents a study on the emission efficiency enhancement of InAsSb nanostructures using a carrier blocking layer. InP is proposed to serve as the carrier blocking layer to suppress the thermal escape of carriers in InAsSb nanostructures and significantly enhance their emission efficiency at high temperature (good photoluminescence signal even at 330 K). However, this leads to a blueshift in their emission wavelength due to the significantly increased quantum confinement of the nanostructures. By inserting a thin InGaAs layer between InP blocking layer and InAsSb nanostructures, longer emission wavelength can be maintained. This provides an approach to achieve InAsSb nanostructures with both good high-temperature optical characteristics and long emission wavelength, which is very useful for fabricating mid-infrared emitters operating at room temperature. © *2010 American Institute of Physics*. [doi:10.1063/1.3436562]

InP-based InAsSb nanostructures have attracted much attention in recent years due to their potential as mid-infrared emitters (2–3 μm region), which have a wide range of applications in military, telecommunications, molecular spectroscopy, biomedical surgery, environmental protection, and manufacturing industry applications.[1–5] Some work has been devoted to the direct growth of InAsSb nanostructures by Stranski–Krastonow method, and flat InAsSb quantum dots (QDs) with high density can be achieved by using InGaAs buffer layer and proper growth parameters.[5–8] Further, by using InGaAsSb sandwich layers the emission wavelength of InAsSb nanostructures can be extended well beyond 2 μm despite their small island height.[9] Unfortunately, the emission efficiency of these InAsSb/InP nanostructures is much lower than that of InAs/InP QDs, especially at high temperatures. The low emission efficiency is mainly caused by the thermal escape of carriers in InAsSb nanostructures due to the low confinement barrier of InGaAs layers. To achieve their ultimate application in mid-infrared emitters, the emission efficiency of these InAsSb nanostructures at high temperature must be enhanced substantially. In this work, a carrier blocking layer (CBL) with wide band gap is proposed to suppress the thermal escape of carriers in InAsSb nanostructures and enhance their emission efficiency.[10] By using InP material as the CBLs, the emission signal of InAsSb nanostructures can be clearly observed up to 330 K in contrast to the 170 K for structures without InP CBL. Meanwhile, the mid-infrared emission wavelength (above 2 μm) is also maintained by tuning the location of InP CBL.

InAsSb nanostructures were grown on semi-insulating InP (001) substrates in a horizontal flow metal-organic chemical vapor deposition reactor (AXI200/4) at a pressure of 180 mbar. Trimethylindium (TMIn), trimethylgallium (TMGa), trimethylantimony (TMSb), PH_3, and AsH_3 were used as the precursors and ultrahigh purity H_2 as the carrier gas. The InAsSb nanostructures were grown using the following layer sequence: first, a 100 nm InP layer and 100 nm InP/$In_{0.53}Ga_{0.47}As$ matrix layer were deposited at 650 °C, then the temperature was dropped to 550 °C to grow 5 nm $In_{0.53}Ga_{0.47}As_{0.25}Sb_{0.75}$ buffer layer and 0.6 nm GaAs interlayer. The temperature was dropped further to 480 °C to grow 4 monolayer of $InAs_{0.5}Sb_{0.5}$ nanostructure layer which was immediately capped with 5 nm $In_{0.53}Ga_{0.47}As$ without any growth interruption. After that the temperature was ramped up to 550 °C to grow 5 nm of $In_{0.53}Ga_{0.47}As_{0.25}Sb_{0.75}$ capping layer, and then the temperature was ramped up again to 650 °C and a 100 nm $In_{0.53}Ga_{0.47}As$/InP/$In_{0.53}Ga_{0.47}As$ spacer layer was deposited. The same steps were followed to grow a top layer of $InAs_{0.5}Sb_{0.5}$ nanostructures for atomic force microscopy (AFM) measurements. The schematic structures of the samples are shown in Fig. 1. During the growth of InAsSb and InGaAsSb layers both the TMSb and AsH_3 sources were introduced simultaneously with group III precursors. To study the effect of the location of InP CBL on the optical properties of InAsSb nanostructures, the thickness distribution of InP and InGaAs materials in the 100 nm InP/InGaAs matrix layer and 100 nm InGaAs/InP/InGaAs spacer layer were varied for different samples, the details of which are given in Table I. The morphology of the top InAsSb nanostructures was characterized by using AFM in tapping mode. Photoluminescence (PL) measurements were carried

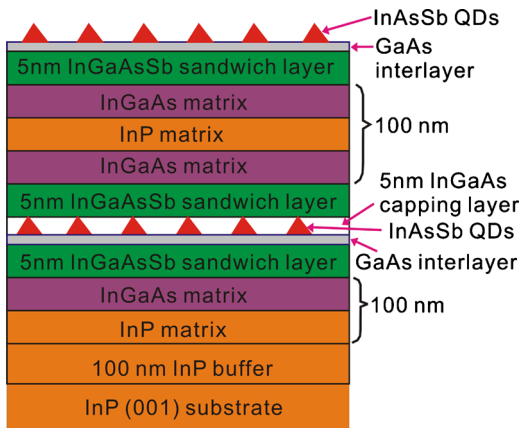

FIG. 1. (Color online) Schematic structure of sample A, B, C, D, and E.

[a]Electronic mail: wen.lei@anu.edu.au.

TABLE I. InP and InGaAs thickness distribution in the 100 nm InP/InGaAs matrix layer and 100 nm InGaAs/InP/InGaAs spacer layer of sample A, B, C, D, and E.

Sample	InP/InGaAs matrix layer thickness distribution (nm)	InGaAs/InP/InGaAs spacer layer thickness distribution (nm)
A	0/100	50/0/50
B	100/0	0/100/0
C	95/5	5/90/5
D	90/10	10/80/10
E	80/20	20/60/20

out under excitation by a 637 nm laser diode. The luminescence signal was collected by a liquid nitrogen-cooled extended InGaAs photodetector through a 0.5 m monochromator.

Elongated InAsSb QDs and short InAsSb quantum dashes are formed in both sample A and B, as shown by the AFM images in the inset of Fig. 2(a). The average height of InAsSb nanostructures is around 2.3 nm and 2.5 nm for sample A and B, respectively. Figure 2 shows the PL spectra of sample A and B at 170 and 330 K. The PL signal of sample A can only be observed up to 170 K, while that of sample B can be clearly observed up to 330 K (the upper limit temperature of the cryostat), as shown in Fig. 2(b). At

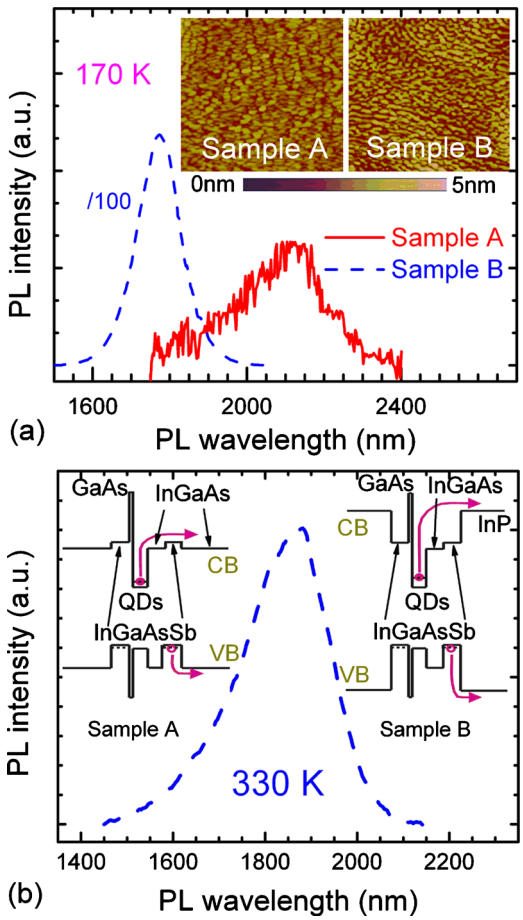

FIG. 2. (Color online) 170 K PL spectra of sample A and B (a), and 330 K PL spectrum of sample B (b). The inset of (a) shows the typical AFM images (1×1 μm^2) of sample A and B; the inset of (b) shows the schematic band diagrams of InAsSb/InGaAsSb nanostructures embedded in InGaAs (sample A) and InP (sample B) matrix.

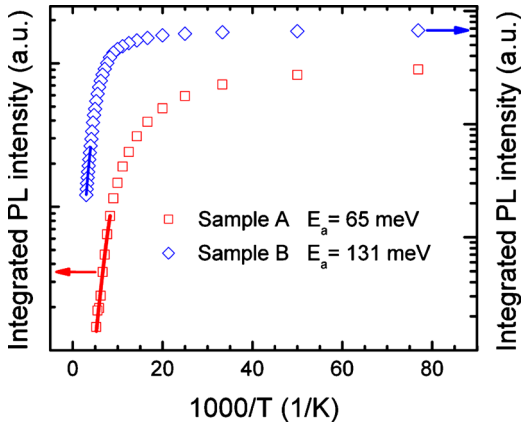

FIG. 3. (Color online) Integrated PL intensity of sample A and B at various temperatures.

170 K the PL intensity of sample B is more than one hundred times that of sample A. All these indicate a significant enhancement of the emission efficiency of InAsSb nanostructures, especially at high temperature. This enhanced emission efficiency for InAsSb nanostructures is mainly caused by the increased carrier confinement induced by InP CBLs, as shown by the schematic band diagrams of sample A and B in the inset of Fig. 2(b).[11] Because the band gap of InP CBLs (1.34 eV at 300 K) is much larger than that of InGaAs (0.74 eV at 300 K),[12] the energy difference between the conduction/valence band edge of InP material and the electron/hole ground state of InAsSb nanostructures is much larger than those between the conduction/valence band edge of InGaAs material and the electron/hole ground state of InAsSb nanostructures. The larger energy differences between the conduction/valence band edge of InP material and the electron/hole ground state of InAsSb nanostructures leads to a high energy barrier for carrier escape and thus effectively enhances their emission efficiency.

To obtain more insight into the PL improvement mechanism of InAsSb nanostructures, temperature dependent PL measurements were performed on sample A and B. Figure 3 shows the integrated PL intensity (I_{PL}) of sample A and B at various temperatures. By using an Arrhenius plot to fit the I_{PL} at high temperatures,[13] the thermal activation energy (E_a) values are determined to be 65 meV and 131 meV for sample A and B, respectively. The significantly larger E_a value of sample B confirms the important role played by InP CBLs. Taking into account the band gap of InGaAs and InP materials, the PL energies of InAsSb nanostructures in sample A and B, and the band-offset between conduction and valence band,[14] the energy difference between the electron ground state in InAsSb nanostructures and InGaAs/InP conduction band edge will be around 92/386 meV, and that between the hole ground state and InGaAs/InP valence band edge will be around 61/257 meV. For sample A, the E_a value fitted agrees well with the energy difference between the ground state of hole and InGaAs valence band edge. This indicates that PL quenching of sample A at high temperatures is mainly dominated by the thermal escape of holes from nanostructures. For sample B, though the E_a value fitted (131 meV) is not as high as the energy barriers introduced by InP CBLs for electrons and holes, it is still much larger than that of sample A. This lower than expected activation energy for sample B might be associated with other issues like dislocations (few

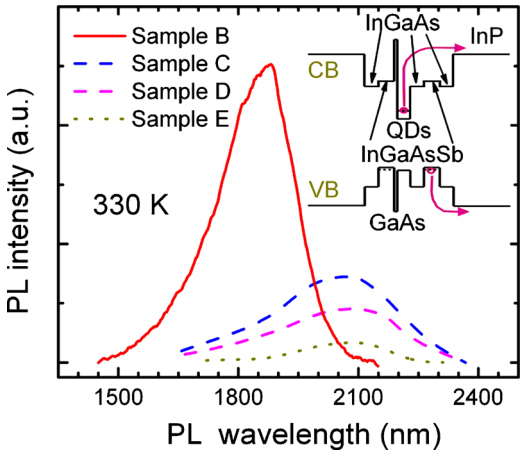

FIG. 4. (Color online) 330 K PL spectra of sample B, C, D, and E. The inset shows the schematic band diagram of InAsSb/InGaAsSb nanostructures embedded in InP matrix with InGaAs insertion layer.

dislocated islands are observed on the surface of sample B with 5×5 μm^2 AFM scan), which is not well understood and remains to be studied further.

As shown in Fig. 2, despite the similar nanostructure size for sample A and B the introduction of InP CBLs leads to a shorter emission wavelength for sample B (2112 and 1780 nm for sample A and B at 170 K, respectively), which is mainly caused by the increased quantum confinement around InAsSb nanostructures. For their ultimate application in mid-infrared emitters, the emission wavelength of InAsSb nanostructures should be maintained above 2 μm. The location of InP CBLs (or the distance between InP CBLs and InAsSb nanostructure layers) provides an effective approach to tune the quantum confinement around InAsSb nanostructures and thus their emission wavelength. In samples C, D, and E, InP CBLs are separated from InGaAsSb sandwich layers by 5, 10, and 20 nm $In_{0.53}Ga_{0.47}As$ layer. As indicated by AFM measurements on sample C, D, and E (images not shown here), elongated InAsSb QDs and short InAsSb dashes are also achieved in these samples. The InAsSb nanostructures have an average height of 2.4, 2.4, and 2.3 nm for sample C, D, and E, respectively. Figure 4 shows the PL spectra of sample B, C, D, and E at 330 K. The emission wavelength of InAsSb nanostructures is extended from 1860 nm for sample B to 2068 nm for sample C, 2082 nm for sample D, and 2085 nm for sample E. The large redshift is mainly caused by the reduced quantum confinement of InP CBLs induced by inserting InGaAs layers between InP CBLs and InGaAsSb layers. The schematic band diagrams of sample C, D, and E are shown in the inset of Fig. 4. With increasing the thickness of InGaAs insertion layer, the distance between InP CBLs and InAsSb nanostructures becomes larger and larger, and the quantum confinement effect of InP CBLs on the electronic structures of InAsSb nanostructures becomes weaker and weaker, leading to the observed redshift in the PL peak. This also leads to a reduced PL intensity for sample C, D, and E, as observed in Fig. 4. But since carrier diffusion lengths in III-V semiconductor (10–100 s of nanometer)[15,16] are more than the thickness of InGaAs insertion layer, InP CBLs in sample C, D, and E can still effectively suppress the thermal escape of carriers in InAsSb nanostructures and leads to the PL signal still being observed at 330 K.

In summary, the high-temperature emission efficiency of InAsSb/InGaAsSb/InGaAs/InP nanostructures has been enhanced significantly by using InP CBLs. InP CBLs is proposed to increase the confinement barrier for carriers, and thus suppress their thermal escape and improve the emission efficiency at high temperature. This leads to good PL signal at 330 K but a shorter emission wavelength due to the increased quantum confinement around InAsSb nanostructures induced by InP CBLs. By inserting a thin InGaAs layer between InP CBL and InAsSb nanostructures to reduce the quantum confinement, both long emission wavelength and high emission efficiency can be achieved for InAsSb nanostructures, which is very useful for the fabrication of mid-infrared emitters operating at room temperature.

Financial support from Australian Research Council (No. DP0774366) is gratefully acknowledged. Facilities used in this work are supported by the Australian National Fabrication Facility.

[1]C. Cornet, F. Doré, A. Ballestar, J. Even, N. Bertru, A. Le Corre, and S. Loualiche, J. Appl. Phys. **98**, 126105 (2005).
[2]Y. Qiu and D. Uhl, Appl. Phys. Lett. **84**, 1510 (2004).
[3]F. Doré, C. Cornet, P. Caroff, A. Ballestar, J. Even, N. Bertru, O. Dehaese, I. Alghoraibi, H. Folliot, R. Piron, A. Le Corre, and S. Loualiche, Phys. Status Solidi C **3**, 3920 (2006).
[4]F. Doré, C. Cornet, A. Schliwa, A. Ballestar, J. Even, N. Bertru, O. Dehaese, I. Alghoraibi, H. Folliot, R. Piron, A. Le Corre, and S. Loualiche, Phys. Status Solidi C **3**, 524 (2006).
[5]W. Lei, H. H. Tan, and C. Jagadish, Appl. Phys. Lett. **95**, 013108 (2009).
[6]K. Kawaguchi, M. Ekawa, T. Akiyama, H. Kuwatsuka, and M. Sugawara, J. Cryst. Growth **291**, 154 (2006).
[7]K. Kawaguchi, M. Ekawa, T. Akiyama, H. Kuwatsuka, and M. Sugawara, J. Cryst. Growth **298**, 558 (2007).
[8]W. Lei, H. H. Tan, and C. Jagadish, Appl. Phys. Lett. **95**, 143124 (2009).
[9]W. Lei, H. H. Tan, and C. Jagadish, "Extending the emission wavelength of InAsSb/InP nanostructures using InGaAsSb sandwich layers" (unpublished).
[10]T. P. Hsieh, P. C. Chiu, J. I. Chyi, H. S. Chang, W. Y. Chen, T. M. Hsu, and W. H. Chang, Appl. Phys. Lett. **89**, 053110 (2006).
[11]The schematic band diagram is drawn with the help of software "NEXTNANO3," http://www.nextnano.de/nextnano3/.
[12]The band-gap energy of InP and $In_{0.53}Ga_{0.47}As$ can be found in the website: http://www.ioffe.ru/SVA/NSM/Semicond/.
[13]W. Lei, Y. H. Chen, Y. L. Wang, B. Xu, X. L. Ye, Y. P. Zeng, and Z. G. Wang, J. Cryst. Growth **284**, 20 (2005).
[14]C. Affentauschegg and H. H. Wieder, Semicond. Sci. Technol. **16**, 708 (2001).
[15]M. Gallant and A. Zemel, Appl. Phys. Lett. **52**, 1686 (1988).
[16]E. Dupuy, D. Morris, N. Pauc, V. Aimez, M. Gendry, and D. Drouin, Appl. Phys. Lett. **94**, 022113 (2009).